Magnetic Resonance Imaging, Vol. 17, No. 9. pp. 1327–1334, 1999
© 1999 Elsevier Science Inc. All rights reserved.
Printed in the USA.
0730-725X/99 $–see front matter

ELSEVIER

PII S0730-725X(99)00061-2

● *Original Contribution*

MAGNETIC RESONANCE IMAGING IN THE EVALUATION OF INFLAMMATORY LESIONS IN MUSCULAR AND SOFT TISSUES: AN EXPERIMENTAL INFECTION MODEL INDUCED BY *CANDIDA ALBICANS*

J. RUIZ–CABELLO,* B. CARRERO–GONZÁLEZ,* P. AVILÉS,† C. SANTISTEBAN,* R.J. MÉNDEZ,‡ J. FERREIRÓS,‡ N. MALPICA,§ A. SANTOS,§ D. GARGALLO–VIOLA,† AND J. REGADERA¶

*NMR Unit and Department of Chemistry–Physics II, Faculty of Pharmacy and ‡Radiodiagnostic Service, San Carlos Clinic Hospital, Complutense University, Madrid 28040, Spain; †Chemotherapy Research Department, GlaxoWellcome, Tres Cantos, Madrid 28760, Spain; §Bioengineering and Telemedicine Group, Madrid Polytechnic University, Madrid 28040, Spain; and ¶Department of Morphology, School of Medicine, Madrid Autonomous University, Madrid, Spain

We have developed an experimental model to monitor inflammatory lesions in muscle and soft-tissues during the different stages of the disease by means of Magnetic Resonance Imaging (MRI). MRI of mice legs infected with *Candida albicans* was performed by standard two-dimensional spin echo and fast spin echo (RARE) using customized coils. The MRI findings were compared with pathologic examinations at the initial acute and established acute inflammatory stages, which provided accurate and detailed information on the evolution of the processes involved. The yeast caused inflammation within the first hours post-inoculation, appearing on T_2-weighted images as an inhomogeneous mass with increased signal intensity. The presence of fungal hyphae was observed as hypointense signal areas in both T_2 and T_1 weighted images, with histologic confirmation. Areas of decreased signal intensity on T_2 weighted images were apparent on the last experimental day and were attributed to the granulation tissue located within the capsule surrounding the abscess. The close correlation found between MRI and histopathology suggests that MRI is an ideal radiologic technique for monitoring the clinical and therapeutic follow-up of fungal infections in muscle and soft tissues. © 1999 Elsevier Science Inc.

Keywords: **Muscles; Soft tissues; Infectious diseases; Yeast; *Candida albicans*.**

INTRODUCTION

Magnetic Resonance imaging (MRI) provides a great deal of information on normal and pathologic tissues based on relative changes in signal intensity when employing different imaging parameters. Thus, MRI can be successfully used to study both initial infection and established acute infections, as well as abscesses, due to its established capability to evaluate different lesions and disease courses.[1–5] Previous studies have evaluated the usefulness of MRI in the follow-up of inflammatory diseases in muscles and other soft tissues.[6–15]

Candida albicans is a major opportunistic pathogen that most frequently infects mucosal surfaces (mouth, vagina, and esophagus). However, once access has been gained to the bloodstream, *C. albicans* can cause lesions in several organs and tissues, including muscle. In this sense, myocarditis and skeletal muscle infections have been reported in patients with disseminated candidiasis and leukemia,[16,17] respectively. Furthermore, muscle infections induced by *C. albicans* have been described in experimental animal models for characterizing immune response to fungal infections,[18,19] to study the pathologic behavior of this microorganism,[20] and to assay the tissue distribution of antifungal agents.[21]

In our opinion, a crucial aspect of any new study using MRI is to emphasize the correlation of MRI findings to the histopathological course. The aim of the present study is to investigate the inflammatory lesions in muscle and soft tissues caused by *C. albicans* in the

RECEIVED 11/14/98; ACCEPTED 5/27/99

Part of the present work was presented as a slide session at the 38th Interscience Conference on Antimicrobial Agents and Chemotherapy, San Diego, CA. USA. 24–27 September 1998.

Address correspondence to Dr. Jesús Ruiz-Cabello, Unidad de RMN, Universidad Complutense de Madrid, Paseo Juan XXIII, 1. Madrid 28040, Spain. E-mail: ruizcabe@eucmax.sim.ucm.es

different stages of the disease in immunocompetent mice. This will not only provide more accurate and detailed information, but will also contribute to define the role of MRI in the correct diagnosis of these diseases. The evolution of the disease was assessed in different stages of infection up to 6 days post-inoculation by histologic methods and MRI, using an experimental high field (4.7 T) system and very homogeneous customized birdcage coils.

MATERIALS AND METHODS

Animals

Male CD-1 non-immunosuppressed mice weighing approximately 30 g (Charles River France Inc. Lyou, France) were used throughout the study. The animals were housed in cages of 10 mice each, with access to food and water ad libitum. The research complied with both national legislation and company policy on the care and use of animals, and with related codes of practice.[22]

Thigh Infection

Candida albican 4711E obtained from the Glaxo-Wellcome culture collection (Grennford, GlaxoWellcome Laboratories, UK) was used throughout. For inoculation in mice, *C. albicans* 4711E was grown on Sabouraud dextrose agar (SDA, Difco, Detroit, USA) plates at 30°C for 48 h. After incubation, cells were harvested, washed in sterile saline, and suspended in sterile saline to a final density of 10^9 CFU/mL. The inoculum size was verified by quantitative culture of serial ten-fold dilutions on SDA plates. Animals were then anesthetized with Halothane (1–1.5%) and intramuscularly (i.m.) inoculated with 100 μL of *C. albicans* blastospores solution (infecting concentration 10^8 CFU/thigh) in the right thigh.[23,24] One hundred μL of sterile saline were i.m. injected into the contralateral thigh as healthy control.

Magnetic Resonance Imaging

Imaging was performed on a Bruker Biospec 47/40 spectrometer (Karlsruhe, Germany) equipped with unshielded gradients with a maximum gradient strength of 300 mT/m. The radio frequency probe used was a customized circular birdcage type resonator operating in the single-coil transmit/receive mode. This coil is a low-pass (8 columns) design consisting of two plastic cylinders: the outer cylinder acts as a shield to diminish receiver losses, improving the SNR and decreasing radiation losses that increase with the resonance frequency, while the inner cylinder functions as an animal holder. We used a printed circuit board and Oxley non-magnetic variable capacitors (0–20 pf) with a large quality factor Q. A double-layer adhesive copper foil was also used to shield the outer tube. For matching and balancing the system, we used both a capacitive circuit and a $\lambda/4$ transformer made with bazooka cable (Belden Wire & Cable Co., Richmond, IN, USA). The diameter (27 mm) and the length (40 mm) allowed simultaneous imaging of the two thighs. Once the coil was prepared and tuned, the quality factor was measured at 200 MHz using a radiofrequency network analyzer HP8712C (Hewlett-Packard, Santa Clara, CA, USA). The resonator had a Q factor to 110 when unloaded, versus 90 when loaded with a phantom (a 0.5 mm diameter sphere filled with distilled water).

For reproducible positioning in subsequent sessions and immobilization during the experiment, the animals were placed in a Plexiglas cradle with a controlled heating blanket, and anesthetized with Halothane (1–1.5%). The two legs were inserted side-by-side in the plastic holder (a syringe tube), which in turn fitted within the resonator, followed by insertion into the magnet.

Serial MRI studies of mice infected with *C. albicans* were made with each animal, adopting multi-section spin echo and fast spin echo sequences, at different stages of infection ranging from Days 0 to 6 post-inoculation. Coronal localization was assessed by a rapid acquisition relaxation enhancement (RARE) sequence with 1544/80 (repetition time msec/echo time ms), 256×256 matrix, 4 cm field-of-view (FOV) and 2 mm slice thickness. Then, 2D and 3D sets of axial images were longitudinally acquired in the axial plane on Day 0, 2, 4, and 6 after injection in a group of animals ($n = 5$), and on Day 1, 3 and 5 in the other group ($n = 5$); the mice were subsequently sacrificed.

The MRI parameters used were: 1) 2D sequences: 20 sections, 1.5-mm thickness, no gap, 256×256 matrix, 3 cm FOV. Both T_1-weighted images with 700/15, one excitation using a multi-slice spin echo sequence, and T_2-weighted images with 3463/76, four excitations using a RARE sequence, were routinely acquired; and 2) 3D sequence: A $128 \times 256 \times 32$ data matrix was used in combination with a $40 \times 40 \times 22$ mm FOV. T_2-weighted images with 2000/67.5, one excitation, using a RARE sequence were acquired.

MRI Analytical Criteria for Infection

MR images were visually evaluated with the following criteria: 1) increase in size of the infected limb in relation to the contralateral limb (control); 2) areas of increased signal intensity of the thigh soft tissues were compared with the contralateral limb on T_2-weighted images. These ill-defined soft tissue lesions were regarded as myositis and panniculitis (cellulitis); and 3) well-delimited collections of inhomogeneous increased signal intensity on T_2-weighted images, with or without a relatively hypointense peripheral margin, were consid-

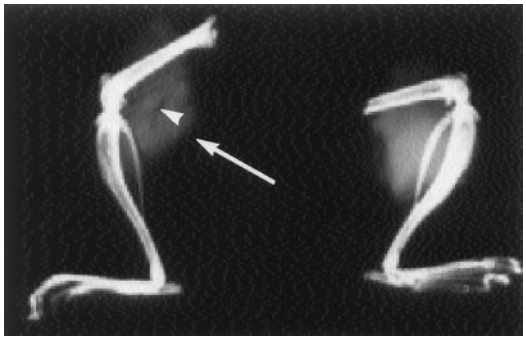

Fig. 1. Radiographic image with ultrafine focus at the site of i.m. injection with *Candida albicans* in both normal and infected limbs. The inoculation site was in the muscular mass of the posterior side of the zeugopod (arrow). Note the muscular disorganization in the infected leg, with formation of a central cavitation (arrowhead).

ered indicative of tissue necrosis and soft tissue abscess formation.

The term hypointense was used to describe the following possibilities: damage appearing with lower signal intensity than healthy muscle on T_1-weighted images, or lesions with a signal intensity lower than or similar to that of healthy muscle on T_2-weighted images.

Pathology

With the aim of establishing a close correlation between the results obtained, we evaluated the following experimental groups of animals: 1) infected mice ($n = 5$) sacrificed on Day 3 (initial acute stage) and 2) infected mice ($n = 5$) sacrificed on Day 6 (well established stage). In both groups, radiologic, macroscopic and histologic lesions were correlated with the MRI results corresponding to the same animal. The infected and contralateral thighs were removed and dissected in parallel slices through the uppermost aspect of the zeugopod. The extremities were placed in a 10% formalin buffered solution for at least 48 h, followed by transversal sectioning at 2 mm intervals along the length of the extremity. Each plane of these slices closely corresponds to the same level of an axial slice in MRI. Plain radiographs (Fig. 1) of both posterior thighs were obtained for the entire piece (2.5 mA, 30 s, 25 KVp) or for the transversal macroscopic sections (2.5 mA, 20 s, 20 KVp) using a Faxitron Series HP43805N X-Ray System (Hewlett-Packard, Santa Clara, CA) with a constant focus-plate distance (25 cm). No fewer than three sections from the infected and control pieces were embedded in paraffin wax for histologic studies. Histologic preparation included staining with hematoxylin and eosin, and the application of histochemical techniques such as Periodic Acid Schiff (PAS) and silver methenamine stains for the detection of fungi.

Statistical Analysis

Volumes of affected tissue were measured regardless of whether the soft tissue was edematous or invaded by abscesses. For each image of every mouse, a region-of-interest (ROI) was manually delimited and volumes were calculated using standard software from Bruker® (Paravision) on 3D T_2-weighted images. ROIs were selected by two different operators who worked blindly with respect to each other. The average of these two measurements is presented. We have tested the null hypothesis $\mu_i = \mu_j$ ($i \neq j$) using data from matched samples by the matched-sample t test, where μ_i and μ_j are these mean values at the Days i and j.

RESULTS

C. albicans caused a strong inflammatory process in the first hours (approximately 4–9 h) after i.m. injection. The abnormalities induced by this microorganism appeared on T_2-weighted images as a moderately to markedly inhomogeneous soft tissue mass with increased signal intensity and extensive diffuse surrounding edema (Fig. 2a), affecting muscles and subcutaneous (s.c.) tissue. This sequence was highly sensitive for the detection of soft tissue inflammatory loci. T_1-weighted images were less demonstrative, showing the soft tissue abnormalities to be characterized by a slightly higher signal intensity than the surrounding non-affected muscles (Fig. 2b).

In this first period, and over the days following fungal inoculation (initial acute inflammatory period), MRI revealed a progressive spread of the affected area characterized by edema and swelling of muscles and soft tissue. Within this region, marked hypointense signal areas on T_2-weighted and T_1-weighted images were present, possibly reflecting necrosis and the presence of *C. albicans* hyphae (Fig. 2, c–e). These MRI alterations were confirmed by the histologic studies. In some cases, the lesions showed a central cavity entirely occupied by yeast cells (Fig. 2f) and surrounded by concentric rings in which yeast concentration progressively decreased toward the periphery. Outside this fungal accumulation, necrotic areas were observed in the muscular fibers and in the s.c. cellular tissue. Other animals showed a necrotic focus with abundant neutrophils but less prominent yeast masses (Fig. 2, g and h). Within these regions, bunches of PAS-positive *C. albicans* hyphae were identified histologically (Fig. 3a). Surrounding these necrotic areas there was a thin inflammatory wall consisting of numerous neutrophils and macrophages (Fig. 3b). These acute inflammatory lesions were diffusely scattered within the endomysial and perimysial connective tissue, destroying the muscular fibers.

The evolution of lesions over one week post-inocula-

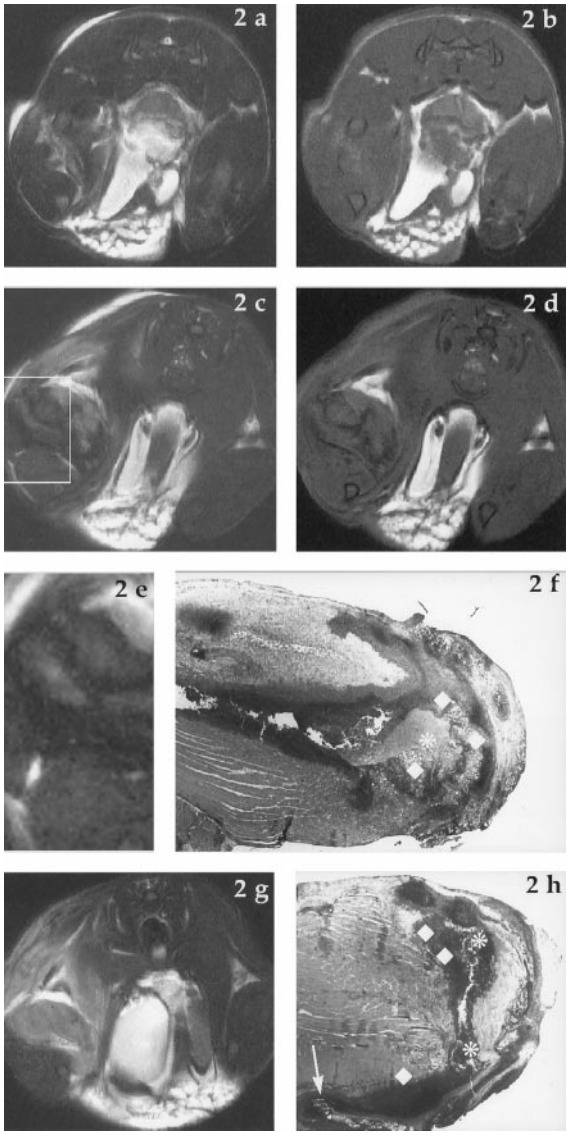

Fig. 2. a, T_2-weighted image (3463/76) of a mouse leg infected with *Candida albicans* at Day 3, showing a mass with increased signal intensity indicating the extension of the edematous area. b, The corresponding T_1-weighted image (700/15) shows a slightly higher signal intensity at the abnormal compared to the non-affected muscles. The affected area is better appreciated with T_2-weighted imaging. c, T_2-weighted image (3463/76) of the same animal in the acute stage, demonstrating an enlarged edematous area and showing different areas of signal void, which probably correspond to masses of yeast cells. d, These hyphal mass accumulations are also distinguished on T_1-weighted images (700/15) e, Zoomed region of image "c." f, This panoramic microscopical image shows a central cavity totally occupied by yeast (*) and surrounded by concentric rings of inflammatory cells (◇), where cellular concentration is seen to progressively decrease toward the periphery. In some animals, both MRI imaging (g) and histologic photomicrographs (h) of a section three days after *C. albicans* inoculation showed a necrotic focus (*) with spreading of the acute inflammation to the muscular fibers (◇) and s.c. cellular tissue (arrow), with a less clear distinction of yeast masses.

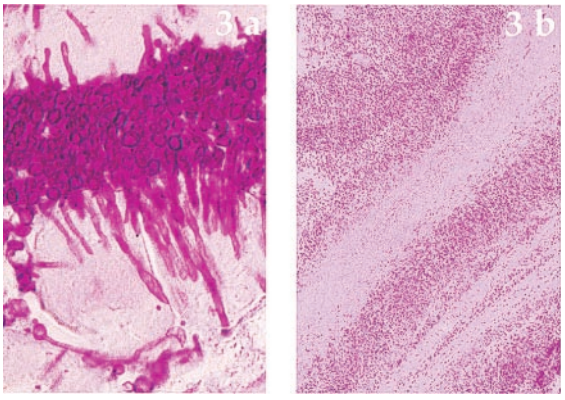

Fig. 3. a, Within the acute lesion, an accumulation of PAS-positive yeast cells and hyphae of *C. albicans* which destroy adjacent muscle fibers is observed. b, Necrotic bands concentrically arranged around the abscessing cavity.

tion was monitored using MRI and both T_1- and T_2-weighted images. The extent of the affected area increased progressively during the acute phase of the infection (Day 0–3), and spread over the fascial planes and muscles into the s.c. tissues and intermuscular fat. These findings were recorded on a daily basis, and affected region volumes were measured using a 3D fast spin echo (Fig. 4). Experimental t-values are shown in Table 1. Significant differences have been found when comparing μ_0 with each one of the other mean values ($j = 1, 2, \ldots, 6$). The greatest t-value obtained ($t = 78.2$; d.f. $= 3$) corresponds to the comparison between the Day 0 and Day 4.

MRI after Day 3 showed these lesions to be generally well-defined inhomogeneous masses, with a signal intensity approximating that of fat on T_2-weighted images (Fig. 5a), and exhibiting an external dark rim which only became clearly evident on Day 6 (Fig. 5a). This may be attributed to the presence of a capsule surrounding the abscess, and not visible on T_1-weighted images (Fig. 5b–d). Areas of decreased signal intensity were apparent within the lesion (Fig. 5a). This corresponded to necrotic contents, as confirmed histologically (Fig. 6a). These areas were also slightly hypointense on T_1-weighted images in all cases. On this last experimental day, histologic study showed a significant reduction of the i.m. necrotic region and a manifest increase in the capsule surrounding the abscess area. This wall was described as a layer of granulation tissue, including abundant lymphocytes, macrophages, and the proliferation of fibroblasts but without the formation of new blood vessels. At the periphery of this band we observed dense chronic inflammatory infiltrates, spreading mainly into the connective tissue surrounding the muscular bundles, and giving rise to myocytolytic reactions (Fig. 6b). In two cases, multiple histiocyte granulomas with a minimal ring of lymphocytes, along with diffuse chronic inflammatory in-

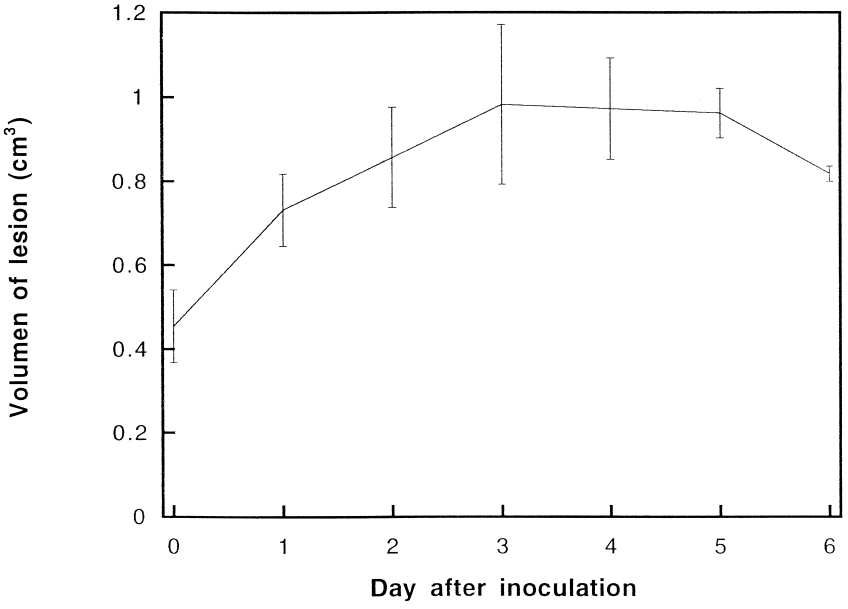

Fig. 4. Evolution of the lesion volume after inoculation with *C. albicans*. The figure represents the mean ± SD of computational measurements performed on Day 0, 2, 4, and 6 after injection in one group of animals ($n = 5$), and on Day 1, 3 and 5 in another group ($n = 5$). The ROIs on each slice of 3D T_2-weighted images were delimited manually by two different operators working blindly to each other.

filtrates, were found in the s.c. adipose tissue. *C. albicans* hyphae were not observed in either myositis or in panniculitis lesions in mice sacrificed 6 days after inoculation.

DISCUSSION

MRI is a relatively new technique in the field of non-invasive clinical diagnostic and experimental animal models. Clinical MRI systems are sometimes used for studying large,[25] and even small domestic animals.[26,27] However, the size of the animal in combination with low signal-to-noise and contrast-to-noise ratios limits the research potential of standard clinical imaging systems in small animal (rat and mouse) experiments, particularly when dedicated radiofrequency coils are not available.[26] MRI studies of myositis in mice were carried out with a strong magnet (4.7 Tesla) possessing a small bore size, though similar results can be obtained with lower field magnets when using high resolution coils specially designed to detect pathologic alterations in small areas.[26] For the purposes of this study, we preferred to examine the entire leg by placing it in a cylindrical extremity coil, in which the signal is homogenous across the image.

Table 1. Statistical values for the evolution of the lesion volume after inoculation with *C. albicans*

	Days					
Days	1	2	3	4	5	6
0	17.9†	9.6†	5.6*	78.2†	12.1†	9.3*
1		n.s.	5.6*	9.7*	8.5*	n.s.
2			n.s.	5.8*	5.3*	n.s.
3				n.s.	n.s.	n.s.
4					n.s.	5.0*
5						−5.1*

Values of the *t*-test obtained from the experimental data. Significant differences: (*) $p < 0.05$, (†) $p < 0.01$, and (n.s.) non-significant.

The selection of pulse sequences for our particular examination was based on the biophysical characteristics of the muscular and soft tissues, and on the suspected pathology (myositis, panniculitis, edema, abscess, etc.). Compared to other soft tissues, normal skeletal muscle has an intermediate to slightly long T_1 relaxation time and a short T_2 relaxation time—though some muscles (e.g., the semimembranous proprius muscle) exhibit greater T_2 (and T_1) values than others, and so are easily distinguishable.[15,28] In contrast, all acute muscle injuries such as inflammation, tumors, etc., have been shown to prolong the T_1 and T_2 relaxation times of the injured tissues.[15,29] The efficacy of the spin echo technique has been firmly established in various musculoskeletal applications at a clinical level,[30,31] and it seems that the image contrast is not qualitatively affected at high field intensities.[32] As was expected, T_2-weighted fast spin echo imaging in the axial plane was particularly helpful for outlining the specific location of lesions and for moni-

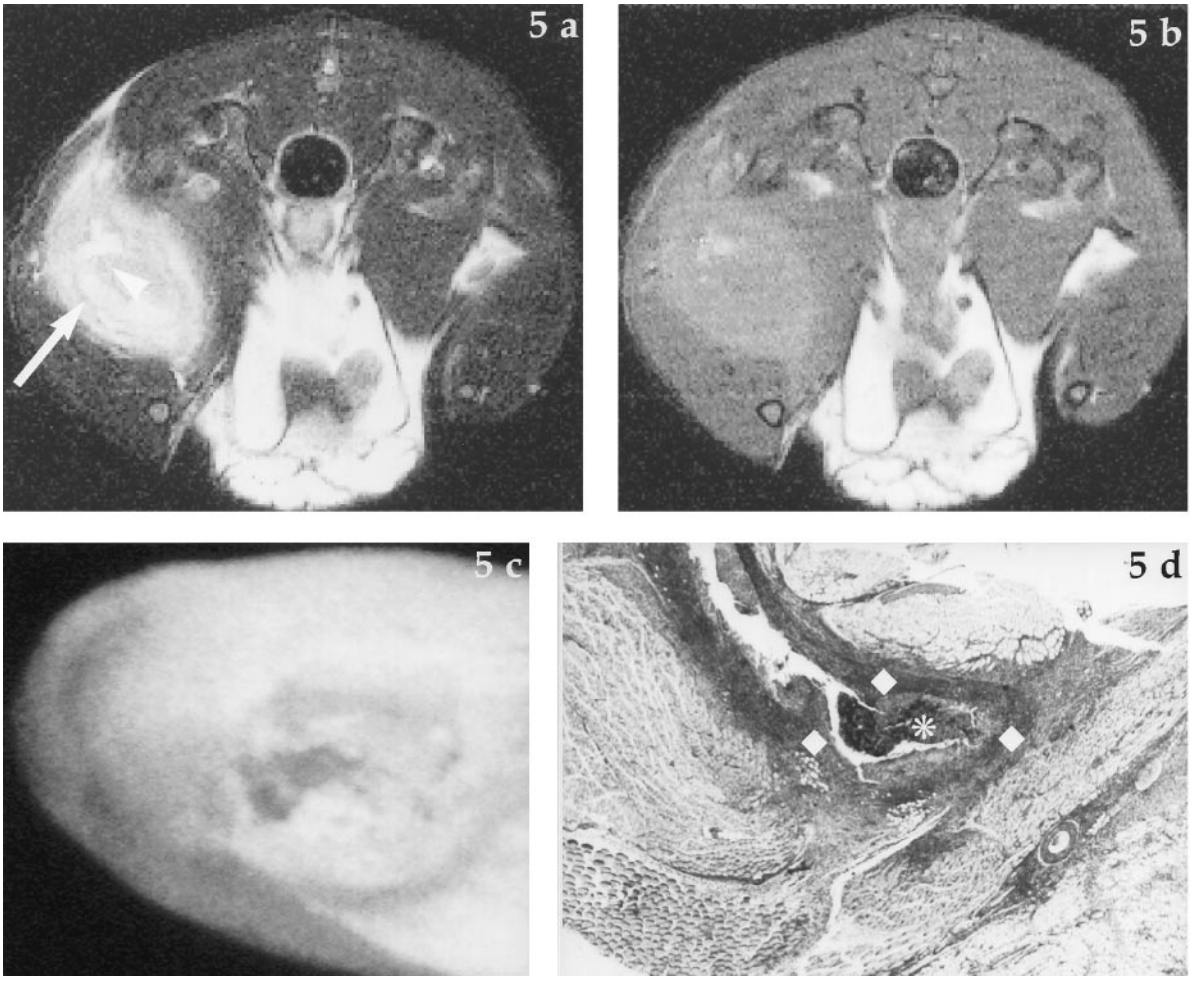

Fig. 5. *C. albicans* myositis model in mouse at Day 6 post-inoculation. a, T_2-weighted image (3463/76) of the thighs showing a well-defined inhomogeneous mass, with a hypointense capsule (arrow) delimiting a central focus of heterogeneous high signal intensity (indicating abscess formation) and necrosis (arrowhead). b, T_1-weighted image (700/15) of the thighs. The lesion exhibits a slightly higher signal intensity, and the capsule is isointense with the muscles. c, Macroscopic slice displaying the different lesions at Day 6 post-inoculation. The image corresponds to the gray-scale digitized output of the original color photograph (after conversion to a 256-tone gray scale) analyzed by NIH Image software. d, Photomicrograph of a section 6 days after inoculation of the yeast, showing a necrotic mass (*) surrounded by a rim of granulation tissue (◇).

toring the extent of the disease. Thus, we observed an increase in signal intensity on T_2-weighted images within the swollen area, a few hours after inoculation (approximately 4–9 h). In contrast, T_1-weighted images were less sensitive in depicting soft tissue abnormalities, since most pathologic processes have long T_1 relaxation times[15] similar to that of normal muscle. However, they were highly specific in distinguishing low intensity signals probably corresponding to hyphal masses of *C. albicans*, as has been demonstrated pathologically. Thus, the histologic findings in the acute stage in some animals undoubtedly provided evidence of fungal balls; these balls contained growing yeast masses, surrounded by concentric layers with progressively lower yeast concentrations. MRI occasionally showed the presence of a large central cavity, presumably occupied by yeasts. In some animals, T_2-weighted images likely displayed different intensity areas suggesting features very consistent with the histologic findings. This apparent correlation was optimized under an optical magnification closer to MRI spatial resolution.

Only on Day 6 after inoculation did we obtain MRI evidence in all mice of a thin, relatively hypointense rim of the abscess wall on T_2-weighted images. Histologically, this structure was described as a layer of granulation tissue containing abundant lymphocytes, macrophages, and the proliferation of fibroblasts but without the formation of new vessels and representing a repair response beginning in the preserved margins of the abscess following an inflammatory reaction.[33] We did not

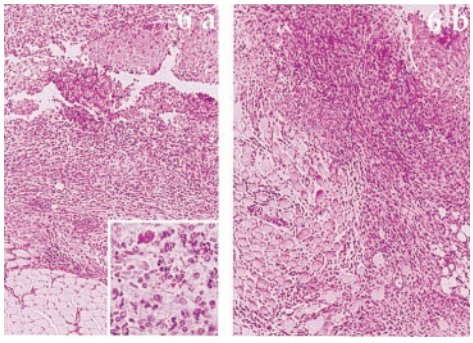

Fig. 6. a, Microabscess with a necrotic center surrounded by acute and chronic inflammation, observed in the well-established acute stage. In the inset, a detail of the necrosis with the presence of abundant leukocytes is shown. b, Necrotizing acute inflammation located at the cavity of muscular tissue. Peripherally, note the dense infiltrations of lymphocytes and plasma cells in the interstice of skeletal muscular cells leading to myocytolytic reactions.

observe a high-intensity rim on T_1-weighted images such as that reported by other authors in musculoskeletal inflammations[10,13] and other lesions.[4,6,34] This hyperintensity on T_1-weighted images within this layer has been attributed to the presence of focal areas of fresh hemorrhage,[4] which were not detected in any of our experiments. Other authors[35] have found abscess capsules to be isointense with muscles on T_1-weighted images, and intraveneous gadolinium infusion has been seen to improve the detection of a vascularized rim in the periphery of muscle abscesses in a study of i.m. abscess induced in rats. Fleckenstein et al.[10] suggested that a hyperintense rim was not observed on T_1-weighted images because of the unspecified origin of bacterial abscesses in those experiments (induced with fecal pellets) though this was not our case. Another possible explanation could be the differences in image contrasting at 4.7 T versus 0.35 T[35] or 1.5 T.[4] Very few data are available with regard to the musculoskeletal system at high field intensities;[32,36] nevertheless, some studies have shown that although numerous quantitative changes are observed, these changes in relaxation times do not qualitatively affect image contrasting on T_1- and T_2-weighted images.[32]

It is well known that *C. albicans* induces a consistent, self-limiting infection suitable for immunologic investigations, where mice survive and recover after 4 to 6 weeks.[18] In our experience two periods could be defined: initial acute and well established acute inflammation. The present study only addressed the progressing acute lesion period, for it is in this stage when the evaluation of therapy is required. Furthermore, during the last period (Day 6 of acute infection), physiological changes in muscle and surrounding areas could have negative effects upon antifungal distribution, and thus impair in vivo antifungal activity.

One of the foremost advantages of noninvasive techniques such as MRI is that they allow the development of reproducible and experimental non-lethal models for evaluating in vivo antifungal activity. Furthermore, MRI allows sequential studies of each particular animal rather than of large groups. Sequential MRI experiments involving the same animals provide better evidence of the pathologic process. Such studies permit each animal to be used as its own control, as a result of which the need for large numbers of animals to secure relevant information is clearly reduced. On the other hand, the noninvasive and non-destructive nature of MRI facilitates the saving of laboratory animals. Finally, inter-individual differences are clearly visible by MRI and can thus be taken into account in the context of ongoing experiments.

In conclusion, MRI is an excellent tool for the noninvasive monitoring of inflammatory lesions in experimental animal muscles and soft tissues, as has been demonstrated in a model of infection induced by *C. albicans*. We have found characteristic low signal intensity areas on T_2- and T_1-weighted images in the acute phase of infection, corresponding to an accumulation of microorganisms within the abscess (as confirmed histologically). We have also detected intrinsic areas of low signal intensity on T_2-weighted images in the well-established acute stage, relating to a granulation tissue capsule surrounding the abscess. The fact that a strong correlation was observed between the MRI data and histologic findings can be used to study the course or nature of the infection in humans suffering from abscesses in these tissues. Our aim is for the present study to be used in future work as the basis for monitoring different therapeutic procedures or approaches.

Acknowledgments—The authors acknowledge the Spanish *Comisión Interministerial de Ciencia y Tecnología* (CICYT) for funding (PB91–0368 and BIO97–0543). Thanks are also due to Margarita Izquierdo Ph.D., Inmaculada Santos Ph.D., and Francisco Martinez-García M.D., for their contribution to this project. Lastly, the authors thank Rosaura San Román, Palmira Villa and Marien Fernández for their excellent technical assistance.

REFERENCES

1. Allegrini, P.R.; Wachsmuth, E.D. Course of murine leukemia retrovirus infection determined in vivo by magnetic resonance imaging. Lab. Invest. 63:568–575; 1990.
2. Chandnani, V.P.; Beltran, J.; Morris, C.S.; et al. Acute experimental osteomyelitis and abscesses: Detection with MR imaging versus CT. Radiology 174:233–236; 1990.
3. Mendez, R.J.; Schiebler, M.L.; Outwater, E.K.; Kressel, H.Y. Hepatic abscesses: MR imaging findings. Radiology 190:431–436; 1994.
4. Ha, H.K.; Lim, G.Y.; Cha, E.S.; et al. MR imaging of tubo-ovarian abscess. Acta. Radiol. 36:510–514; 1995.

5. Pui, M.H.; Chang, S.K. Comparison of inversion recovery fast spin-echo (FSE) with T_2-weighted fat-saturated FSE and T_1-weighted MR imaging in bone marrow lesion detection. Skeletal Radiol. 25:149–152; 1996.
6. Wall, S.D.; Fisher, M.R.; Amparo, E.G.; Hricak, H.; Higgins, C.B. Magnetic resonance imaging in the evaluation of abscesses. Am. J. Roentgenol. 144:1217–1221; 1985.
7. Beltran, J.; Noto, A.M.; McGhee, R.B.; Freedy, R.M.; McCalla, M.S. Infections of the musculoskeletal system: High field strength MR imaging. Radiology 164:449–454; 1987.
8. Paajanen, H.; Brasch, R.C.; Schmiedl, U.; Ogan, M. Magnetic resonance imaging of local soft tissue inflammation using gadolinium-DTPA. Acta. Radiol. 28:79–83; 1987.
9. Tang, J.S.H.; Gold, R.H.; Basset, L.W.; Seeger, L.L. Musculoskeletal infection of the extremities: Evaluation with MR imaging. Radiology 166:205–209; 1988.
10. Fleckenstein, J.L.; Burns, D.K.; Murphy, F.K.; Jayson, H.T.; Bonte, F.J. Differential diagnosis of bacterial myositis in AIDS: Evaluation with MR imaging. Radiology 179:653–658; 1991.
11. Rahmouni, A.; Chosidow, O.; Mathieu, D.; et al. MR imaging in acute infectious cellulitis. Radiology 192:493–496; 1994.
12. Kransdorf, M.; Temple, H.T.; Sweet, D.E. Focal myositis. Skeletal Radiol. 27:283–287; 1998.
13. Hovi, I.; Valtonen, M.; Korhola, O.; Hekali, P. Low-field MR imaging for the assessment of therapy response in musculoskeletal infections. Acta. Radiol. 36:220–227; 1995.
14. Loh, N.N.; Ch′en, I.Y.; Cheung, L.P.; Li, K.C.P. Deep fascial hyperintensity in soft-tissue abnormalities as revealed by T_2-weighted MR imaging. Am. J. Roentgenol. 168:1301–1304; 1996.
15. El–Khoury, G.Y.; Brandser, E.A.; Kathol, M.H.; Tearse, D.S.; Callaghan, J.J. Imaging of muscle injuries. Skeletal Radiol. 25:3–11; 1996.
16. Odds, F.C. Candida and Candidiasis. London: Balliere Tindall; 1988.
17. Diggs, C.H.; Eskenasy, G.M.; Sutherland, J.C.; Wiernik, P.H. Fungal infection in muscle in acute leukemia. Cancer 38:1771–1772; 1976.
18. Pearsall, N.N.; Lagunoff, D. Immunological responses to *Candida albicans*. I. Mouse-thigh lesion as a model for experimental candidiasis. Infect. Immun. 9:999–1002; 1974.
19. Tabeta, H.; Mikami, Y.; Abe, F.; Ommura, Y.; Arai, T. Studies on defense mechanism against *Candida albicans* infection in congenitally athymic nude (nu/nu) mice. Mycopathol. 84:107–113; 1983.
20. Ashman, R.B.; Fulurija, A.; Robertson, T.A.; Papadimitriou, J.M. Rapid destruction of skeletal muscle fibers by mycelial growth forms of *Candida albicans*. Exp. Mol. Pathol. 62:109–117; 1995.
21. Fischman, A.J.; Alpert, N.M.; Livni, E.; et al. Pharmacokinetics of ^{18}F-labeled Fluconazole in rabbits with candidal infections studied with positron emission tomography. J. Pharmacol. Exp. Ther. 259:1351–1359; 1991.
22. Institute of Laboratory Animal Resources, Commission on Life Sciences, National Research Council. In: Guide for the care and use of laboratory animals. Washington, DC: National Academy Press; 1996.
23. Hunter, P.A.; Rolinson, G.N.; Witting, D.A. Comparative activity of amoxicillin and ampicillin in an experimental bacterial infection in mice. Antimicrob. Agents Chemother. 4:285–293; 1973.
24. Vogelman, M.; Gudmundsson, S.; Turnige, J.; Legget, J.; Craig, W.A. In vivo post-antibiotic effect in a thigh infection in neutropenic mice. J. Infect. Dis. 157:287–298; 1988.
25. Secrist, R.D.; Traynelis, V.; Schochet, S.S. MR imaging of acute cortical venous infarction: Preliminary experience with an animal model. Magn. Reson. Imaging 7:149–153; 1988.
26. Wolf, R.F.E.; Lam, K.H.; Mooyaart, E.L.; Bleichrodt, R.P.; Nieuwenhuis, P.; Schakenraad, J.M. Magnetic resonance imaging using a clinical whole body system: An introduction to a useful technique in small animal experiments. Lab. Animals 26:222–227; 1992.
27. Brown, M.S.; Kornfeld, M.; Mun–Bryce, S.; Sibbit, R.R.; Rosenberg, G.A. Comparison of magnetic resonance imaging and histology in collagenase induced hemorrhage in the rat. J. Neuroimag. 5:23–33; 1995.
28. Bonny, J.M.; Zanca, M.; Boespflug–Tanguy, O.; Dedieu, V.; Joandel, S.; Renou, J.P. Characterization in vivo of muscle fiber types by magnetic resonance imaging. Magn. Reson. Imaging 16:167–173; 1998.
29. Herfkens, R.; Davis, P.; Crooks, L.; et al. Nuclear magnetic resonance imaging of the abnormal live rat and correlations with tissue characteristics. Radiology 141:211–218; 1981.
30. Rubin, D.A.; Kneeland, J.B. MR Imaging of the musculoskeletal system: Technical considerations for enhancing image quality and diagnostic yield. Am. J. Roentgenol. 163:1155–1163; 1994.
31. Burk, D.L.; Dalinka, M.K.; Shiebler, M.L.; Cohen, E.K.; Kressel, H.Y. Strategies for musculoskeletal magnetic resonance imaging. Radiol. Clin. North Am. 26:653–672; 1988.
32. Duewell, S.H.; Ceckler, T.L.; Ong, K.; et al. Musculoskeletal MR imaging at 4 T and at 1.5 T: Comparison of relaxation times and image contrast. Radiology 196:551–555; 1995.
33. Luna, M.A. Candidiasis. In: D. H. Connor, F. W. Chandler, (Eds). Pathology of Infectious Diseases, Vol. 2. Connecticut: Appleton & Lange, 1997: pp. 953–964.
34. Rihs, J.D.; Padhye, A.A.; Good, C.B. Brain abscess caused by Schizophyllum commune: An emerging basidiomycete pathogen. J. Clin. Microbiol. 34:1628–1632; 1996.
35. Paajanen, H.; Grodd, W.; Revel, D.; Engelstad, B.; Brasch, R.C. Gadolinium-DTPA enhanced MR imaging of i.m. abscess. Magn. Reson. Imaging 5:109–115; 1987.
36. Chen, J.H.; Avram, H.E.; Crooks, L.E.; Arakawa, M.; Kaufman, L.; Brito, A.C. In vivo relaxation times and hydrogen density at 0.063–4.85 T in rats with implanted mammary adenocarcinomas. Radiology 184:427–434; 1992.